

## $Q^2$ -dependent parametrizations of parton distribution functions

D. W. Duke and J. F. Owens

*Physics Department, Florida State University, Tallahassee, Florida 32306*

(Received 14 November 1983)

We have used a large set of high- $Q^2$  data on deep-inelastic scattering, dimuon mass distributions, and  $J/\psi$   $x_F$  distributions to extract estimates of the  $Q^2$ -dependent quark and gluon distribution functions in nucleons. The  $Q^2$  dependence of these functions is parametrized in a manner convenient for predicting a large variety of reactions for  $Q^2 \simeq 4-200$  (GeV/c) $^2$  and for extrapolation to the ultrahigh values of  $Q^2$  that will be probed by future accelerators in the TeV energy range.

### I. INTRODUCTION

The accumulation in recent years of high-quality data on deep-inelastic structure functions for lepton-nucleon scattering has made available fairly reliable information on the individual quark distributions in nucleons.<sup>1</sup> However, information on the gluon distribution function is considerably harder to obtain and one must rely on rather indirect methods for its determination. The gluon distribution mixes with the quark flavor-singlet distribution and thereby influences the  $Q^2$  evolution of the quark distributions. While this allows one to put constraints upon the gluon distribution, it does not result in a direct measurement. This situation has resulted in a larger level of uncertainty for the gluon than is associated with the various quark distributions.

Another source of uncertainty is associated with the correlation between the QCD scale parameter  $\Lambda$  and the shape of the gluon distribution. A soft (hard) gluon distribution results in a relatively smaller (larger) preferred value of  $\Lambda$  (Refs. 2 and 3). Arbitrarily changing  $\Lambda$  independently of the gluon distribution can give rise to very misleading results and potentially unreliable predictions for very-high-energy processes. On the contrary, if this correlation is taken into account, it turns out that gluon distributions which are initially quite different often end up giving rather similar predictions for many hard-scattering processes.

Apart from deep-inelastic scattering, many interesting reactions receive substantial contributions from gluon-initiated subprocesses, e.g., heavy-quark production, high- $p_T$  particle and photon production, etc. The large uncertainty attached to the gluon distribution often results in wide variations in theoretical predictions for these processes, especially if an extrapolation over a wide kinematic range is being performed. Predictions for proposed high-energy accelerators are particularly sensitive to this problem.

The purpose of this paper is to present useful estimates for the  $Q^2$ -dependent parton distributions within the nucleon using data from a variety of reactions. The  $Q^2$  dependence has been calculated only to leading-logarithm accuracy, which is certainly sufficient for most needs. Two different gluon distributions have been used, reflecting the current uncertainty in the determination of the

precise shape of the gluon distribution. In the next section the data selection and the fitting procedures will be briefly discussed. In Sec. III some simple parametrizations of the results are presented. In Sec. IV some comparisons are made to a variety of data sensitive to gluon-initiated hard-scattering subprocesses. In addition, we offer some final discussion of our results and a brief comparison to previously available parametrizations.

### II. DATA SET AND FITTING PROCEDURE

In obtaining the sets of parton distributions presented here we considered three distinct types of data: deep-inelastic structure functions, dimuon mass distributions, and  $J/\psi$   $x_F$  distributions. The deep-inelastic data set consisted of a representative sample of neutrino,<sup>4</sup> muon,<sup>5</sup> and electron<sup>6</sup> data from a variety of targets. Although this choice does not exhaust the supply of available data, it is sufficient for our purposes. The relative normalizations of the various experiments were allowed to vary (without penalty) within the normalization uncertainties of the various experiments. For both of the fits discussed below, we somewhat arbitrarily chose to normalize everything to the European Muon Collaboration (EMC) hydrogen data. Relative to this data the SLAC, CERN-Dortmund-Heidelberg-Saclay (CDHS), and EMC deuterium data were multiplied by factors of 0.923 (0.946), 1.124 (1.118), and 1.052 (1.053) for the soft (hard) gluon choices as discussed below.

The least-squares fits were made with four flavors of quarks and it was assumed that the charmed sea of the nucleon was zero at the input value of  $Q_0^2 = 4$  (GeV/c) $^2$ . This simple treatment is, of course, not correct near the charm-quark production threshold and could therefore lead to an overestimate of the charm contribution to the low- $x$  scaling violations. Accordingly, cuts of  $x \geq 0.1$  and  $Q^2 \geq Q_0^2$  were imposed. An additional cut of  $W^2 \geq 10$  GeV $^2$  was imposed in order to avoid possible complications from target mass corrections and higher twist effects.

The information concerning the sea-quark distributions in deep-inelastic scattering comes mainly from the low- $x$  region which is sensitive to the charm content mentioned above as well as to the precise assumptions made for  $R = \sigma_L / \sigma_T$ . In order to further constrain the sea it was

decided to include in the fitting procedure data for high-mass dimuon production. Specifically, data from both Fermilab<sup>7</sup> and the CERN ISR<sup>8</sup> for  $s^{3/2} d\sigma/dM dy$  for  $|y| < 0.1$  have been used. In order to avoid possible backgrounds from heavy-quark semileptonic decays<sup>9</sup> a cut on the dimuon mass of  $M \geq 6 \text{ GeV}/c^2$  was imposed. Furthermore, the normalization of the data was allowed to vary in order to account for, among other things, the well known  $K$ -factor effect upon leading-logarithm calculations.<sup>10</sup> The  $K$  factors determined by the fits were 1.91 (1.74) for the soft (hard) gluon choices as discussed below.

The data discussed above are sensitive to the gluon distribution only through mixing with the quark singlet terms. In order to have some data which are more sensitive to the gluon distribution, we have also considered the  $x_F$  distributions of  $J/\psi$ 's produced in  $pN$  collisions.<sup>11</sup> The "duality"-type model was used in fitting these data as discussed in Ref. 12. The inclusion of these data places a strong constraint on the gluon distribution, but the price to be paid is the use of a model rather than a theoretical calculation for  $J/\psi$  production. Accordingly, these  $J/\psi$  data were used in only one of the fits to be discussed below.

### III. PARTON-DISTRIBUTION FITS

The two fits to be presented here differ chiefly in the shape of the gluon distribution. In each case a form

$$xG(x, Q_0^2) = A_G(1 + \gamma_G x)(1 - x)^{\eta_G} \quad (1)$$

was used. The first set was determined using all three of the data types discussed in Sec. II. The parameter  $A_G$  was fixed by the momentum sum rule while  $\gamma_G$  and  $\eta_G$  were fitted. These parameters are very highly correlated and the errors are large if both are varied at once. In the final fit the values were fixed at  $\gamma_G = 9.0$  and  $\eta_G = 6.0$ , values which were typical of the fitted results and are similar to those suggested by earlier analyses.<sup>13,14</sup> The valence-quark distributions were parametrized by

$$\begin{aligned} x(u_V + d_V) &= N_{ud} x^{\eta_1} (1 - x)^{\eta_2} (1 + \gamma_{ud} x), \\ x d_V &= N_d x^{\eta_3} (1 - x)^{\eta_4} (1 + \gamma_d x), \end{aligned} \quad (2)$$

where

$$\begin{aligned} N_{ud} &= 3 / \{ B(\eta_1, \eta_2 + 1) [1 + \gamma_{ud} \eta_1 / (\eta_1 + \eta_2 + 1)] \}, \\ N_d &= 1 / \{ B(\eta_3, \eta_4 + 1) [1 + \gamma_d \eta_3 / (\eta_3 + \eta_4 + 1)] \}, \end{aligned}$$

and  $B(x, y)$  is the Euler beta function. For the sea quarks we assumed simply

$$x\bar{u} = x\bar{d} = x\bar{s} = A_S(1 - x)^{\eta_S} S / 6. \quad (3)$$

The fitted parameter values at  $Q_0^2 = 4 \text{ (GeV}/c^2)^2$  may be obtained from the  $s=0$  values of the  $Q^2$ -dependent parametrization given below. The fitted value of  $\Lambda$  in the leading order is  $0.2 \text{ GeV}/c$ . Hereafter this set of input distributions will be referred to as "set 1."

The gluon parameters in set 1 are directly constrained by the  $J/\psi$  data and indirectly but still strongly constrained by the dimuon data. This latter circumstance arises because the  $pN$  dimuon data are proportional to the antiquark distributions and these are in turn strongly in-

fluenced through evolution by the gluon distribution. It could be argued that the  $pN$  dimuon data may be influenced by anomalous nuclear<sup>15</sup> effects which could alter the form of the sea.<sup>16</sup> Accordingly, a second fit was performed without the  $J/\psi$  and Columbia-Fermilab-Stony Brook (CFS) dimuon data. For this fit the gluon parameters were chosen to be  $\gamma_G = 9.0$  and  $\eta_G = 4.0$ , thus corresponding to an intentionally broader gluon distribution. The fitted value of  $\Lambda$  for this case is  $0.4 \text{ GeV}/c$ , illustrating the previously mentioned  $\Lambda$ -gluon correlation.

The fitting program<sup>17</sup> used in these analyses operates by directly integrating the Altarelli-Parisi equations in  $x$  space. This is a fast and convenient way to obtain the evolved distributions during the fitting, but for subsequent applications it is more convenient to have simple  $Q^2$ -dependent parametrizations of the results. Similar to most previous analyses<sup>18</sup> we have fitted functional forms depending on the variable

$$s = \ln[(\ln Q^2 / \Lambda^2) / (\ln Q_0^2 / \Lambda^2)]$$

to the evolved distributions. The resulting parametrizations may be trusted at the few-percent level for  $Q^2$  up to about  $1 \text{ (TeV}/c)^2$  for the bulk of the  $x$  range 0 to 1. The only exception to this is for the gluon and sea distributions at large- $x$  values where the distributions are already extremely small.

The level of agreement between the exact and fitted values of the singlet quark and gluon distributions at very small  $x$  is an issue of some relevance to QCD predictions for, e.g., a  $20 \text{ TeV} \times 20 \text{ TeV}$  collider. In this scenario production of a  $Q\bar{Q}$  pair via  $gg$  fusion with  $m_Q \leq 35 \text{ GeV}/c^2$  would probe the gluon distribution in the region  $x = 2m_Q / \sqrt{s} \leq 2 \times 10^{-3}$ . This is well inside the QCD-generated small- $x$  spike of width  $\Delta x = 0.05$  in the gluon distribution. As a measure of the reliability of our fits at very small  $x$ , we note that for  $Q^2 \approx 5000 \text{ (GeV}/c)^2$  and  $x = 0.0014$ , the gluon fit is about 14% (27%) higher than the result of the numerical integration for the set 1 (set 2) distributions, respectively. For the singlet quark distributions the corresponding values are 4% and 20.5%. For  $x > 0.005$  and  $Q^2 \leq 1 \text{ (TeV}/c)^2$ , the discrepancies are nowhere more than a few percent and should be quite reliable, except, as stated above, for the gluon distribution for  $x > 0.8$  and  $Q^2$  in the  $1 \text{ (TeV}/c)^2$  range.

On the other hand, the physical significance of those spikes in the singlet quark and gluon distributions is quite problematical. The spikes result from an  $n = 1$  pole in the singlet anomalous-dimension matrix and it is by no means certain whether this leading-logarithm behavior survives a more careful treatment. This then results in up to an order-of-magnitude uncertainty in those QCD predictions which probe very small  $x \leq 10^{-3}$ .

The valence distributions are parametrized as in Eqs. (1) and (2) and  $xG$ ,  $xS$ , and  $xc$  are parametrized in the general form

$$Ax^a(1-x)^b(1+ax+\beta x^2+\gamma x^3), \quad (4)$$

where  $S = 2(\bar{u} + \bar{d} + \bar{s})$ . Each of the constants in all of the parametrizations has a quadratic dependence on the variable  $s$  of the form  $A(s) = A_0 + A_1 s + A_2 s^2$ , etc.

The results for set 1 are as follows. For  $x(u_V + d_V)$

and  $xd_V$  [see Eqs. (1) and (2)],

$$\begin{aligned}\eta_1 &= 0.419 + 0.004s - 0.007s^2, \\ \eta_2 &= 3.46 + 0.724s - 0.066s^2, \\ \gamma_{ud} &= 4.40 - 4.86s + 1.33s^2, \\ \eta_3 &= 0.763 - 0.237s + 0.026s^2, \\ \eta_4 &= 4.00 + 0.627s - 0.019s^2, \\ \gamma_d &= -0.421s + 0.033s^2;\end{aligned}$$

for  $xS$  [see Eq. (4)],

$$\begin{aligned}A &= 1.265 - 1.132s + 0.293s^2, \\ a &= -0.372s - 0.029s^2, \\ b &= 8.05 + 1.59s - 0.153s^2, \\ \alpha &= 6.31s - 0.273s^2, \\ \beta &= -10.5s - 3.17s^2, \\ \gamma &= 14.7s + 9.80s^2;\end{aligned}$$

for  $xc$  [see Eq. (4)],

$$\begin{aligned}A &= 0.135s - 0.075s^2, \\ a &= -0.036 - 0.222s - 0.058s^2, \\ b &= 6.35 + 3.26s - 0.909s^2, \\ \alpha &= -3.03s + 1.50s^2, \\ \beta &= 17.4s - 11.3s^2, \\ \gamma &= -17.9s + 15.6s^2;\end{aligned}$$

for  $xG$  [see Eq. (4)],

$$\begin{aligned}A &= 1.56 - 1.71s + 0.638s^2, \\ a &= -0.949s + 0.325s^2, \\ b &= 6.0 + 1.44s - 1.05s^2, \\ \alpha &= 9.0 - 7.19s + 0.255s^2, \\ \beta &= -16.5s + 10.9s^2, \\ \gamma &= 15.3s - 10.1s^2.\end{aligned}$$

For set 2 we find the following. For  $x(u_V + d_V)$  and  $xd_V$  [see Eqs. (1) and (2)],

$$\begin{aligned}\eta_1 &= 0.374 + 0.014s, \\ \eta_2 &= 3.33 + 0.753s - 0.076s^2, \\ \gamma_{ud} &= 6.03 - 6.22s + 1.56s^2, \\ \eta_3 &= 0.761 - 0.232s + 0.023s^2, \\ \eta_4 &= 3.83 + 0.627s - 0.019s^2, \\ \gamma_d &= -0.418s + 0.036s^2;\end{aligned}$$

for  $xS$  [see Eq. (4)],

$$\begin{aligned}A &= 1.67 - 1.92s + 0.582s^2, \\ a &= -0.273s - 0.164s^2,\end{aligned}$$

$$\begin{aligned}b &= 9.15 + 0.530s - 0.763s^2, \\ \alpha &= 15.7s - 2.83s^2, \\ \beta &= -101s + 44.7s^2, \\ \gamma &= 223s - 117s^2;\end{aligned}$$

for  $xc$  [see Eq. (4)],

$$\begin{aligned}A &= 0.067s - 0.031s^2, \\ a &= -0.120 - 0.233s - 0.023s^2, \\ b &= 3.51 + 3.66s - 0.453s^2, \\ \alpha &= -0.474s + 0.358s^2, \\ \beta &= 9.50s - 5.43s^2, \\ \gamma &= -16.6s + 15.5s^2;\end{aligned}$$

for  $xG$  [see Eq. (4)],

$$\begin{aligned}A &= 0.879 - 0.971s + 0.434s^2, \\ a &= -1.16s + 0.476s^2, \\ b &= 4.0 + 1.23s - 0.254s^2, \\ \alpha &= 9.0 - 5.64s - 0.817s^2, \\ \beta &= -7.54s + 5.50s^2, \\ \gamma &= -0.596s + 0.126s^2.\end{aligned}$$

When using these parametrizations it is necessary to remember that  $\Lambda=0.2$  GeV/ $c$  for set 1 and  $\Lambda=0.4$  GeV/ $c$  for set 2 have been determined by least-squares fits to be the optimum values implied by the data and the other assumptions discussed above. Significant alterations in  $\Lambda$  will yield potentially misleading results as will be discussed in the next section.

#### IV. DISCUSSION

We shall first discuss some of the more important features of our two sets of distributions and then briefly compare our results with some of the earlier published results.

In Fig. 1 the gluon distributions from sets 1 and 2 are shown at  $Q_0^2=4$  (GeV/ $c$ )<sup>2</sup>. The difference in character between the hard and soft distributions is clearly evident. In Fig. 2 the distributions are again compared, this time after evolution to  $Q^2=90$  (GeV/ $c$ )<sup>2</sup>. Below  $x=0.3$  there is now very little difference between the two curves. The data points are estimates of the gluon distribution based on fits of the duality model to data for  $\Upsilon$  production.<sup>19</sup> The measurements agree best with the distributions from set 1. In Fig. 3 the  $J/\psi$   $x_F$  distribution data<sup>11</sup> used in the fit for set 1 are shown together with the set 1 and set 2 predictions for  $Q^2=9$  (GeV/ $c$ )<sup>2</sup>. Again the results for set 1 are in better agreement with the data. However, the theoretical uncertainties associated with the duality model preclude the possibility of making a definite choice between the two sets at this time.

In Fig. 4 the fits to the dimuon data<sup>7</sup> are shown. They appear to be nearly identical although there is actually a

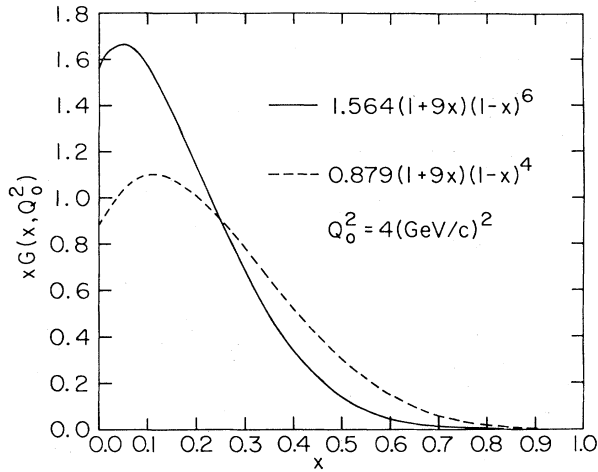


FIG. 1. The set 1 (solid curve) and set 2 (dashed curve) gluon distributions at  $Q_0^2 = 4 \text{ (GeV/c)}^2$ .

significant increase in  $\chi^2$  for set 2 (dashed curve) which is not apparent in the figure due to the fact that the errors on the CFS data are smaller than the plotted points in most cases. This significance would be decreased if systematic normalization errors were also included. It should of course be noted that there may well be anomalous (from the point of view of the parton model) nuclear target effects on the sea quarks<sup>16</sup> which would seriously compromise any attempts to compare these data with deep-inelastic structure functions. This is an important but unanswered question at this time. Again, it would be premature to choose between the distributions on the basis of the dimuon data.

In Fig. 5 some results for high- $p_T$   $\pi^0$  production<sup>20</sup> are shown. For these data the  $\pi^0$ 's were reconstructed from completely resolved  $\gamma$ 's. Accordingly, no high- $p_T$  direct

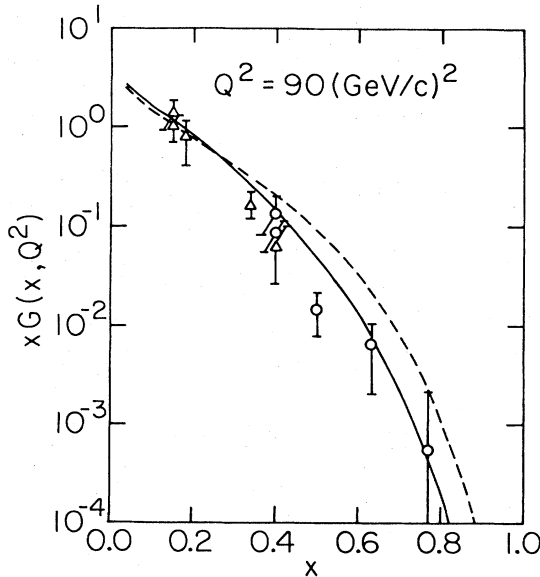


FIG. 2. The set 1 (solid curve) and set 2 (dashed curve) gluon distributions evolved to  $Q^2 = 90 \text{ (GeV/c)}^2$ . The data are from Ref. 19.

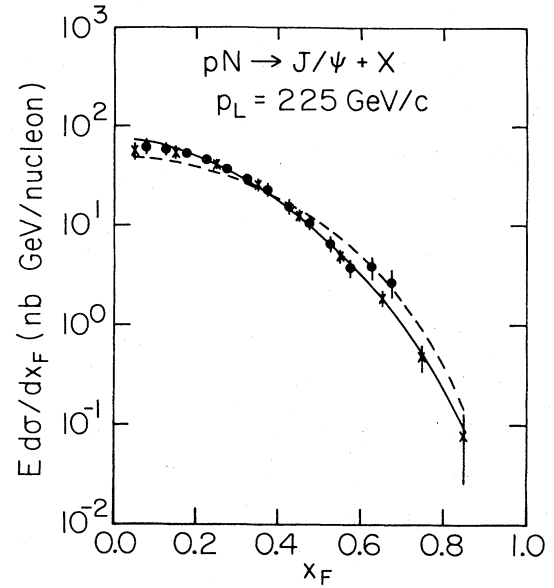


FIG. 3. The predictions for the  $x_F$  distribution of  $J/\psi$ 's produced in  $pN$  collisions based on the set 1 (solid curve) and set 2 (dashed curve) distributions. The data are from Ref. 11.

or bremsstrahlung photon contributions were added. The definition of  $Q^2$  used here was

$$Q^2 = 2\hat{s}\hat{t}\hat{u}/(\hat{s}^2 + \hat{t}^2 + \hat{u}^2),$$

where a caret is used to denote the Mandelstam variables

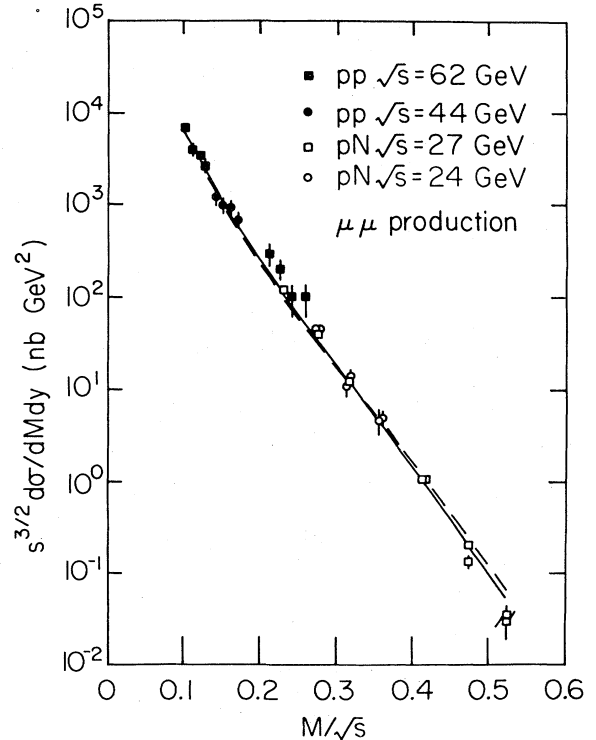


FIG. 4. The set 1 (solid curve) and set 2 (dashed curve) predictions for muon pair production. The data are from Ref. 7 (open circles and squares) and Ref. 8 (closed circles and squares).

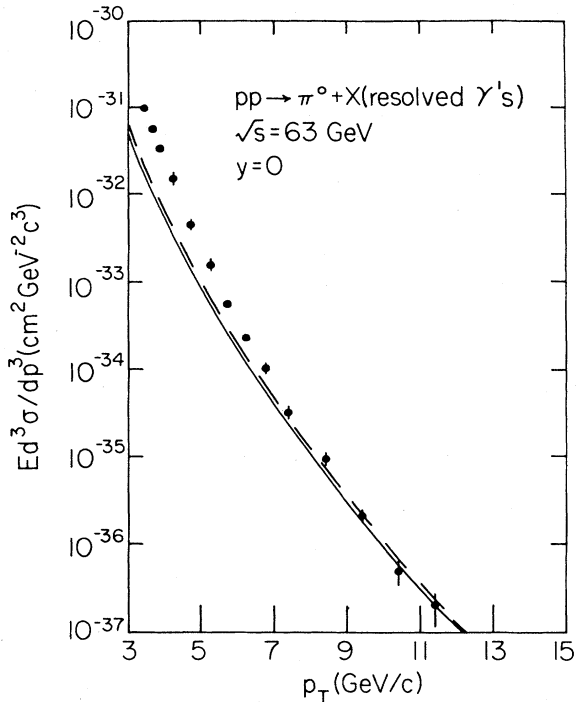


FIG. 5. The set 1 (solid curve) and set 2 (dashed curve) predictions for  $\pi^0$  production at large  $p_T$ . The data from Ref. 20.

for the parton scattering subprocess. The two curves are strikingly similar, due in part to the  $\Lambda$ -gluon correlation. The set 1 predictions are decreased relative to those for set 2 at all  $p_T$  as a result of the smaller value of  $\Lambda$  (and hence  $\alpha_s$ ). However, at small  $p_T$  part of this reduction is made up for by the larger gluon distribution at small  $x$ . At high  $p_T$  again some of the reduction is made up for by the less rapid scaling violations implied by the smaller value of  $\Lambda$ . In fact, the quark-quark scattering term has a crossover at  $p_T \simeq 13$  GeV/c with the set 1 prediction being larger at higher  $p_T$  values. At  $p_T$  values below 7 GeV/c both sets underestimate the data. The inclusion of some parton- $k_T$  smearing in a model-dependent fashion would increase the predictions in this region. At values of  $p_T$  above about 7 GeV/c both sets are in reasonable agreement with the data shown. The differences are smaller than the typical normalization errors between the different experiments.

In Fig. 6 the predictions of both sets are compared with some high- $p_T$  inclusive  $\gamma$  data.<sup>20</sup> These data have been corrected for various triggering biases and correspond to fully inclusive (as opposed to “direct”) photons. Accordingly, a bremsstrahlung contribution has been added using the leading-logarithm QCD prediction for the photon fragmentation function. At  $p_T = 9$  GeV/c this is only a small contribution of about 20%. Again, it is interesting to note that the two sets of predictions are very similar. The difference is slightly larger than for the  $\pi^0$  case since the dominant subprocess here is  $qg \rightarrow \gamma q$ .

A comparison has also been made between the recent UA2 jet-production data<sup>21</sup> and leading-logarithm QCD predictions based on both sets of distributions. The pre-

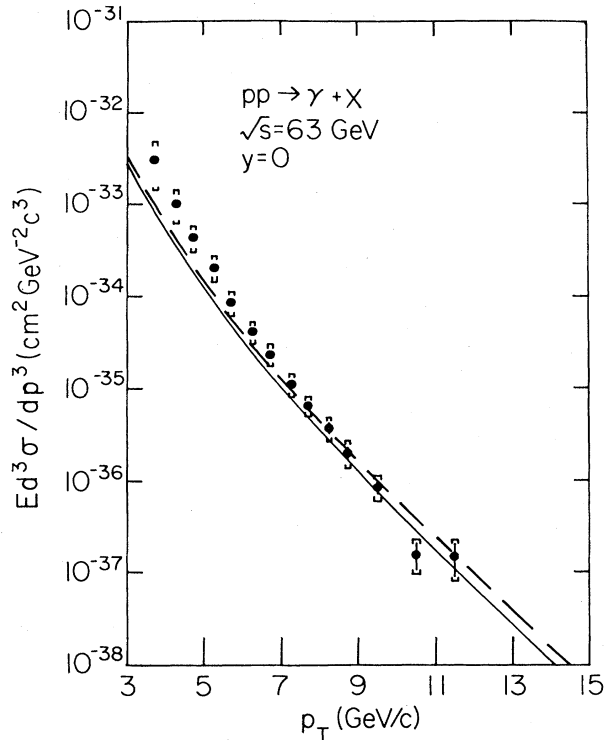


FIG. 6. The set 1 (solid curve) and set 2 (dashed curve) predictions for direct photon production at large  $p_T$ . The data are from Ref. 20.

dictions agree well with the shape of the data, falling slightly below them, but within the overall quoted systematic error. These data extend to  $p_T = 138$  GeV/c which means that  $Q^2$  values on the order of  $10^4$  (GeV/c)<sup>2</sup> are reached.

There are a number of previously published sets of  $Q^2$ -dependent parton distributions that may be compared to our present ones. The major improvement that we have made is that our sets were determined by fitting to a large set of high- $Q^2$  data rather than particular individual data sets. Thus, we expect our sets to be useful for making predictions both for a wide range of reactions for  $Q^2 \simeq 4 - 200$  (GeV/c)<sup>2</sup> and for extrapolation to the ultrahigh values of  $Q^2$  that will be probed by future machines in the TeV energy range.

The gluon distribution determined<sup>13</sup> by the CDHS collaboration agrees well with our set 1 gluon, both in shape and in  $Q^2$  dependence. Unfortunately, there are no corresponding  $Q^2$ -dependent quark distributions available from the same analysis.

The set of distributions given by Gluck, Hoffman, and Reya<sup>14</sup> (GHR) is most similar to our set 2. The major difference is that GHR use three light flavors in the evolution and calculate the charm contribution directly from the photon-gluon-fusion model<sup>22</sup> (supplemented by slow rescaling<sup>23</sup> for neutrino reactions). We have checked, however, that our set 2 and the GHR set give comparable predictions at least up to the TeV scale.

Another prominently used set of distributions was published by Baier, Engels, and Petersson.<sup>24</sup> This set features

the assumption  $u_V = d_V$ , in rather clear violation of the SLAC data, and a very hard gluon  $xG \propto (1-x)^{2.9}$ , with the exponent determined from an analysis of the second and third gluon moments.<sup>25</sup> This simple method of analysis is only useful for low  $x \leq 0.3$  and yields a totally misleading large- $x$  behavior, as verified by the present and previous<sup>26</sup> analyses. Unfortunately, the predictions for production rates near threshold of heavy particles at high energy are often sensitive to the large- $x$  behavior of the gluon. Such estimates will be even more unduly biased if a small value of  $\Lambda$  is used, since then the gluon will tend to stay large at large  $x$  due to the decreased scaling violations. Finally, one must be particularly careful to heed the caution of Baier, Engels, and Petersson to use their

parametrization only for  $s < 1$ . For  $s > 1$  the gluon parametrization, in particular, shows a violent antiscaling behavior, such that for  $Q^2 \simeq 10^6$  (GeV/c)<sup>2</sup> (characteristic for producing TeV scale masses) the production via  $gg \rightarrow Q\bar{Q}$  of heavy pairs will be overestimated by about an order of magnitude. We have checked that our distributions, on the other hand, are reliable until  $s \simeq 2$ , i.e., safely into the TeV scale range.

#### ACKNOWLEDGMENT

This work was supported in part by the U.S. Department of Energy.

- 
- <sup>1</sup>F. Eisele, in *Proceedings of the 21st International Conference on High Energy Physics, Paris, 1982*, edited by P. Petiau and M. Porneuf [J. Phys. (Paris) Colloq. **43**, 1982].
- <sup>2</sup>R. M. Barnett and D. Schlatter, Phys. Lett. **112B**, 475 (1982).
- <sup>3</sup>A. Devoto, D. W. Duke, J. F. Owens, and R. G. Roberts, Phys. Rev. D **27**, 508 (1983).
- <sup>4</sup>H. Abramowicz *et al.*, Z. Phys. C **17**, 283 (1983).
- <sup>5</sup>J. J. Aubert *et al.*, Phys. Lett. **105B**, 315 (1981).
- <sup>6</sup>A. Bodek *et al.*, Phys. Rev. D **20**, 1471 (1979).
- <sup>7</sup>A. S. Ito *et al.*, Phys. Rev. D **23**, 604 (1981).
- <sup>8</sup>D. Antreasyan *et al.*, Phys. Rev. Lett. **48**, 302 (1982).
- <sup>9</sup>H. G. Fischer and W. M. Geist, Z. Phys. C **19**, 159 (1983).
- <sup>10</sup>G. Altarelli, R. K. Ellis, and G. Martinelli, Nucl. Phys. B **157**, 461 (1979).
- <sup>11</sup>J. G. Branson *et al.*, Phys. Rev. Lett. **38**, 1331 (1977); K. J. Anderson *et al.*, *ibid.* **42**, 486 (1979).
- <sup>12</sup>M. Gluck, J. F. Owens, and E. Reya, Phys. Rev. D **17**, 2324 (1978); V. Barger, W. Y. Keung, and R. J. N. Phillips, Z. Phys. C **6**, 169 (1980).
- <sup>13</sup>H. Abramowicz *et al.*, Z. Phys. C **12**, 289 (1982).
- <sup>14</sup>M. Gluck, E. Hoffmann, and E. Reya, Z. Phys. C **13**, 119 (1982).
- <sup>15</sup>J. J. Aubert *et al.*, Phys. Lett. **123B**, 113 (1983).
- <sup>16</sup>R. L. Jaffe, Phys. Rev. Lett. **50**, 229 (1983); C. H. Llewellyn Smith, Phys. Lett. **128B**, 107 (1983).
- <sup>17</sup>This program is described in some detail in Ref. 3.
- <sup>18</sup>A. J. Buras and K. J. F. Gaemers, Nucl. Phys. **B132**, 249 (1978).
- <sup>19</sup>S. Childress *et al.*, University of Washington report, 1983 (unpublished).
- <sup>20</sup>E. Anassontzis *et al.*, Z. Phys. C **13**, 277 (1982).
- <sup>21</sup>P. Bagnaia *et al.*, report No. CERN-EP/84-12, 1984 (unpublished).
- <sup>22</sup>E. Witten, Nucl. Phys. **B104**, 445 (1976); M. Gluck and E. Reya, Phys. Lett. **83B**, 98 (1979).
- <sup>23</sup>R. M. Barnett, Phys. Rev. Lett. **36**, 1163 (1976).
- <sup>24</sup>R. Baier, J. Engels, and B. Petersson, Z. Phys. C **2**, 265 (1979).
- <sup>25</sup>J. G. H. deGroot *et al.*, Phys. Lett. **82B**, 456 (1979).
- <sup>26</sup>D. W. Duke, J. F. Owens, and R. G. Roberts, Nucl. Phys. **B195**, 285 (1982).